

Earthquake precursors based upon snap-of-a-whip effect.

Michail Zak

Jet Propulsion Laboratory California Institute of technology

Abstract.

The objective of this paper is to analyze thermal anomalies associated with pre-seismic activities, to develop a model that explains effects of relatively fast appearance and disappearance of the ground temperature increases, and to apply that model to several hours prediction of the parameters of a potential earthquake. The approach is based upon the so-called snap-of-a-whip effect when an S-wave penetrates the upper soil/sand layer and releases its potential energy into heat at the very surface. This effect (that mathematically is equivalent to a snap of a whip) has been described by M.Zak, in [1], [2], and [3]. Special discussion is devoted to the inverse problem of prediction of expected earthquake parameters based upon observed time-series as well as to proposed experiment.

1. Introduction.

There are several physical phenomena altered by pre-seismic activity such as soil moisture, gas contain and composition, etc. But the most spectacular and mysterious phenomenon of those mentioned above, is a fast appearance and disappearance of the ground temperature increases several hours prior and up to a day after the earthquake. The confidence in correct values of the surface temperature time series has been recently increased due to techniques of precise co-registration of all satellite scenes developed by N. Bryant, A. Zobrist and T.Logan, [4], and [5].

One of possible explanation of the thermal anomaly was proposed (and supported by experiments) by F.Freund [6] who suggests that satellites may be recording cold luminescence in the thermal infrared, not hot thermal emissivity signatures. However, this theory can hardly be extended to the areas that are covered by a thick layer of soil or sand. But, coincidentally, these particular areas are the most vulnerable to destruction caused by earthquakes. The main purpose of our approach is to propose an explanation of thermal anomalies observed in the areas covered by a thick layer of soil/sand. Although these two theories are based upon different physical phenomena, they actually can complement each other since they are applicable to non-overlapping areas.

2. Seismic S-waves.

The main destructive "weapon" of an earthquake is the wave of shear stress, or S-wave. This wave originated at the fault as a result of a slip phenomenon when the shear stress exceeds the friction stress. Although the accumulation of the potential energy of elastic forces between the earthquakes is relatively slow, the growth of the second gradients of shear stress is significantly accelerated prior to the next earthquake. During this period, S-waves of high second gradients as well as of high accelerations (but still of low amplitudes) start propagating from the fault upward to the ground according to the following equation

$$\rho \frac{\partial^2 u}{\partial t^2} = \frac{\partial}{\partial x} \left(G \frac{\partial u}{\partial x} \right) \quad (1)$$

where ρ is rock density, u is shear displacement, and G is shear modulus of rock. Since $G = \text{const.}$, the wave propagates with the constant characteristic speed

$$v = \sqrt{\frac{G}{\rho}} = 3400 \text{ m sec}^{-1} \quad (2)$$

if $G=3 \times 10^{10}$ Pa and $\rho=2.5 \times 10^3 \text{ kg m}^{-3}$.

If x is a vertical axis, the wave $u = u(x,t)$ approaches a free surface and reflected back thereby spreading any local increase of shear stress over the whole depth. However, if the free surface of the rock is covered by a layer of soil or sand, the wave is only partly reflected, but partly penetrates the soil/sand layer. In order to evaluate the ratio of these two components, one should recall that shear stress in a soil/sand layer is generated by friction. Therefore, the propagating shear stress cannot exceed the friction stress, i.e.

$$\tau \leq \tau_{s \text{ max}} = f_s \gamma_s \quad (3)$$

Here τ is propagating stress, $\tau_{s \text{ max}}$ is maximum friction stress, f_s is coefficient of static friction between rock and soil/sand, and γ_s is the weight of the soil/sand per unit area. If the shear wave $u(x,t)$ is of relatively small amplitude (as was assumed from the very beginning), and therefore, the propagating shear stress does not exceed the maximum friction stress, then there is no slip at the boundary between the rock and soil/sand. Hence, the shear deformation of the rock and of the soil/sand are the same at the boundary, i.e. the corresponding shear stresses as well as the specific energies are proportional to the shear moduli

$$\frac{\tau_s}{\tau} = \frac{G_s}{G} = \frac{E_s}{E} \quad \text{if} \quad \frac{\partial u}{\partial x} = \frac{\partial u_s}{\partial x} \quad \text{at} \quad x = H \quad (4)$$

since,

$$\tau = G \frac{\partial u}{\partial x}, \quad \tau_s = G_s \frac{\partial u_s}{\partial x}, \quad \text{and} \quad E = \tau \frac{\partial u}{\partial x}, \quad E_s = \tau_s \frac{\partial u_s}{\partial x}. \quad (5)$$

where H is the depth of the soil/sand layer, u_s is the shear displacement of soil/sand, G , G_s , E and E_s are shear moduli and specific energies of rock and soil/sand, respectively.

As noticed above, a typical value for the rock shear modulus is $G = 3 \times 10^{10}$ Pa. For the soil/sand layer of 1 km height, the shear modulus at the bottom of the layer $G_s = 0.74 \times 10^7$ Pa. Hence, only about .025% of the total energy of the shear wave penetrates the soil/sand layer, while the most part of the energy returns to the rock via reflection.

Let us turn now to the alternative case when the propagating shear stress exceeds the maximum friction stress, i.e. when

$$\tau > \tau_{s \max} \quad (6)$$

The excessive stress that is defined via the kinematic coefficient of friction f_k

$$\Delta\tau = \tau - f_k \gamma, \quad f_k < f_s \quad (7)$$

cannot be transmitted by the soil/sand medium, and the energy ΔE associated with this stress dissipates into heat via the friction. It should be noticed that this is not the phenomenon we are looking for. Indeed, here the heat is generated at the bottom of the soil/sand layer, and it spreads over the whole layer by the slow mechanism of thermal conductivity. Therefore, the effect of this wave on the surface temperature will be vanishingly small. Instead we are looking for such an elastic wave that penetrate the soil/sand layer and dissipates its energy at the very surface. As will be shown below, such a wave exists, and it is similar to a wave propagating along a whip and producing a snap at the free end due to sharp concentration of energy there, (see Fig.1)

3. Snap-of-a-whip effect.

Let us return to the case (3) when a small portion of the shear wave enters the soil/sand layer without dissipation. Its propagation upwards is still governed by Eq. (1) with the only difference that now the shear modulus depends upon the depth. We will use here the following expression after R. Weigel,[7]:

$$G_s = 0.5\rho_s gx, \quad \rho_s = 1500\text{kgm}^{-3} \quad g = 9.81\text{m sec}^{-2} \quad (8)$$

A modified version of Eq.(1)

$$\frac{\partial^2 u}{\partial x^2} = 0.5g \frac{\partial}{\partial x} \left(x \frac{\partial u}{\partial x} \right) \quad (9)$$

was studied by M.Zak [1,2,3] who showed that this equation has a unique stable solution in the open interval

$$0 < x \leq H \quad (10)$$

that does not include the surface point $x = 0$; however, this solution becomes unstable and non-unique in the closed interval

$$0 \leq x \leq H \quad (11)$$

that includes the surface point $x = 0$.

A physical interpretation of this mathematical result is very simple. It follows from the fact that in a soil/sand medium, the leading front of the shear wave propagates

towards a free surface slower than the trailing front does. As a result of that, the length of the wave tends to zero, while the energy per unit length tends to infinity at the surface. Indeed, let us turn to Eq. (9) and assume that the shear wave approaching the soil/sand is of a rectangular form. (Such an approximation allows one to avoid unnecessary mathematical complications without losing qualitative as well as global quantitative effects). The total energy transmitted by such a wave of length l is

$$E_0 = \frac{1}{2} \int_0^l \left\{ G \left(\frac{\partial u}{\partial x} \right)^2 + \rho \left(\frac{\partial u}{\partial t} \right)^2 \right\} dx = Gu \quad (12)$$

where u is the shear displacement over the total wavelength l . The simplification here is due to the rectangular shape of the wave, and in particular, due to the relationship between the jumps of strains and velocities [3]

$$\left[\frac{\partial u}{\partial t} \right] = \sqrt{\frac{G}{\rho}} \left[\frac{\partial u}{\partial x} \right] \quad (13)$$

After passing through the boundary, the energy of the wave penetrating the soil/sand layer is

$$E_s = G_s u_s = 0.00025 E_0 \quad (14)$$

As noticed above, the rest of the energy will return with the reflected wave. The initial length of the penetrating wave l_s is found from Eq.(14) with the reference to Eq.(4)

$$\frac{\partial u}{\partial x} = \frac{u}{l} = \frac{u_s}{l_s}, \quad l_s = l \frac{u_s}{u} = \frac{E_s G}{G_s E} l = l \quad (15)$$

The penetrating wave continues to propagate upward. First, its speed drops from the value in the rock (see Eq.(2) to the initial value at the boundary

$$v_s(x=H) = \sqrt{\frac{G_s(x=H)}{\rho_s}} = 2100 \text{ m sec}^{-1} \quad (16)$$

Then the speed starts gradually decreasing and approaches zero at the surface

$$v_s = \frac{dx}{dt} = \sqrt{0.5gx}, \quad v_s \rightarrow 0, \quad \frac{\partial v_s}{\partial x} \rightarrow \infty \quad \text{at} \quad x \rightarrow 0 \quad (17)$$

preserving constant deceleration

$$a_s = \frac{dv_s}{dt} = v_s \frac{\partial v_s}{\partial x} = 0.25g \quad (18)$$

However, as follows from Eq.(17), the negative velocity gradient becomes unbounded at the surface; in mathematical language it means violation of the so-called Lipschitz condition, and that causes non-uniqueness of the solutions to Eq.(17) in the interval that includes the free surface. Nevertheless, this mathematical ‘‘formality’’ has a clear physical interpretation that will be given below. Indeed, let us introduce a trajectories of the

leading point x_1 , trailing point x_2 and the middle point x^* of the propagating wave. As follows from Eq.(17):

$$x_1 = (\sqrt{H-l} - 0.5\sqrt{0.5gt})^2 \geq 0 \quad (19)$$

$$x_2 = (\sqrt{H} - 0.5\sqrt{0.5gt})^2 \geq 0 \quad (20)$$

$$x^* = (\sqrt{H-0.5l} - 0.5\sqrt{0.5gt})^2 \geq 0 \quad (21)$$

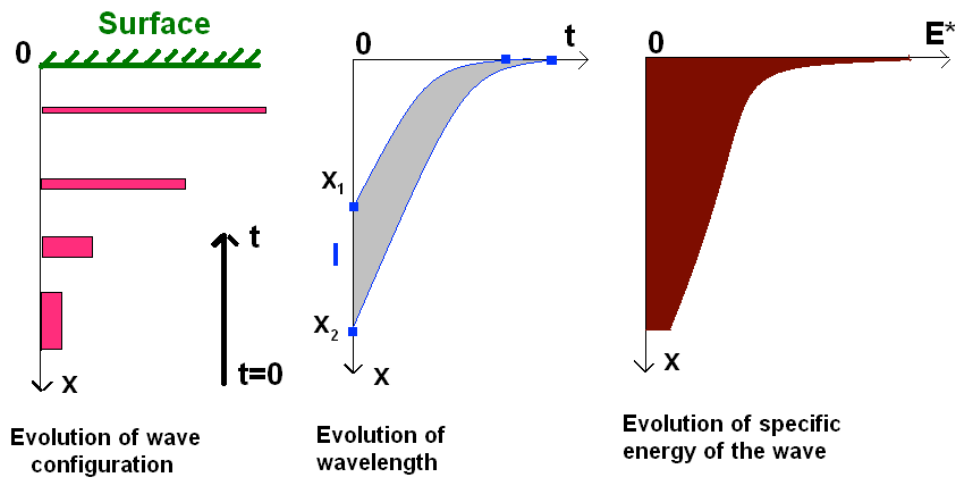


Figure 2. Snap-of-a-whip effect

All these trajectories (known as the characteristics of the original equation (1)) approach the surface $x = 0$ with zero speed (i.e. without reflection) at different times

$$t_1 = \frac{\sqrt{H-l}}{0.5\sqrt{0.5g}} < t^* = \frac{\sqrt{H-0.5l}}{0.5\sqrt{0.5g}} < t_2 = \frac{\sqrt{H}}{0.5\sqrt{0.5g}} \quad (22)$$

Therefore, the wave is not reflected from the surface, but rather stays there, while its length $\Delta l = x_1 - x_2$ gradually decreases from l to 0:

$$\Delta l = l - \sqrt{0.5g}(\sqrt{H} - \sqrt{H-l})t \quad (23)$$

The energy per unit length of the wave becomes unbounded at the surface

$$E^\# = \frac{E_s}{\Delta l} = \frac{E_s}{l - \sqrt{0.5g}(\sqrt{H} - \sqrt{H-l})t} \rightarrow \infty \quad \text{at} \quad x \rightarrow 0 \quad (24)$$

i.e when

$$t = t^{**} = \frac{l}{\sqrt{0.5g}(\sqrt{H} - \sqrt{H-l})} \quad (25)$$

At this time, different solutions of the same differential equation (17) (known as the characteristic equation to the original equation (1)) intersect, and that represents the non-uniqueness of the solution to Eq.(1). The instability of these solutions results from the unboundedness of the specific energy E^* at $x = 0$, $t = t^*$ even if the initial value of this energy at $t = 0$ is arbitrarily small (but finite)

$$E^*(x = H) \ll 1, \quad E^*(x = 0) \rightarrow \infty \quad (26)$$

The behavior of the solution to Eq.(1) is illustrated in Figure2.

4. Energy dissipation.

The evolution of the shear wave described above is not complete: it does not include yet the dissipation of mechanical energy into heat. Actually, there are two different mechanisms of the dissipation. One of them mentioned earlier occurs when shear stress exceeds the friction stress (see Eq. (3)). As a result of that, the elastic energy first transfers into kinetic energy of a slip, and then it dissipates into heat via friction. It should be emphasized that this type of dissipation starts in depth of the soil/sand layer, and therefore, its contribution into the surface temperature is delayed by a slow process of thermal conductivity. Following the same line of argumentation, it is clear that the waves of *higher* intensity contribute *less* into the surface temperature since their dissipation

starts earlier, and therefore, given the same total energy, long shallow waves are more effective in raising the surface temperature. In order to evaluate the second mechanism of dissipation, recall that prior to dissipation, the wave energy is equally divided between the kinetic and potential (stress-based) components (see Eqs. (12) and (13)). Since the shear wave is not reflected from the surface, its kinetic energy eventually transfers to heat as well, but, unlike the previous case, that occurs only at the very surface. That is why the second mechanism is more important for the explanation of the thermal anomaly. The manifestations of this end-effect can be found in observations of a sudden jump of free-surface particles during underground explosions. Similar effect takes place at the free end of a whip when the total energy transfers into heat via a supersonic snap.

Let us analyze the first mechanism of energy dissipation. It starts when the friction stress is equal to the elastic stress

$$\tau_f = f_s \rho g x_f = \sqrt{E^* G_s} = \tau \quad (27)$$

Here x_f is the x-coordinate of the middle of the wave when dissipation starts. With reference to Eqs. (8) and (24), one can rewrite Eq. (27) as

$$x_f = \frac{E_s}{2\sqrt{f_s \rho g} [l - \sqrt{0.5g}(\sqrt{H} - \sqrt{H-l})t_f]} \quad (28)$$

while the time t_f (when the dissipation starts) as a function of x_f , is found from Eq. (21)

$$t_f = \frac{\sqrt{H - 0.5l} - \sqrt{x_f}}{0.5\sqrt{0.5g}} \quad (29)$$

Substituting t_f from Eq. (29) into Eq.(28), one arrives at a cubic equation with respect to x_f . Although the exact solution to this equation is available, we will need only a qualitative result following from that solution, namely, that x_f decreases with increase of the initial length of the shear wave (at a fixed total energy E_s), Fig.3. As shown in this figure, a wave of high intensity, i.e. of high energy per unit length starts dissipating its potential energy earlier than a shallow wave (having the same total energy, but lower energy per unit length). The distribution of the dissipated energy over the soil/sand layer can be written in the following form

$$Q_1 = 0 \quad \text{at} \quad \zeta > \xi_f, \quad Q_1 = 0.5\rho g \zeta \quad \text{at} \quad 0 \leq \zeta \leq \zeta_f \quad (30)$$

Here

$$\zeta = x_2(t) - x_1(t), \quad \zeta_f = x_2(t_f) - x_1(t_f) \quad (31)$$

where x_1 and x_2 as functions of t are given by Eqs. (19) and (20), respectively, and Q_1 is the dissipated energy per unit length.

The energy dissipated into heat via the second mechanism is equal to the energy of the wave at the surface, and it can be expressed as a δ -function

$$Q_2 = (E_s - \int_{\zeta} Q_1 d\zeta) \delta(\zeta \rightarrow 0) \quad (32)$$

The total dissipated energy per unit length is

$$Q = Q_1 + Q_2 \quad (33)$$

One can verify that the total energy dissipated into the whole soil/sand layer is equal to E_s i.e. to the initial energy of the wave.

The temperature T of the soil/sand layer heated by the dissipated energy is described by the non-homogeneous equation of thermal conductivity complemented by the corresponding initial and boundary conditions

$$\frac{\partial T}{\partial t} = \kappa \frac{\partial^2 T}{\partial x^2} + \frac{Q}{c\rho_s}, \quad (34)$$

$$T(x,0) = T_0, \quad T(H,t) = T_0, \quad \frac{\partial T}{\partial x}(0,t) = -\lambda[(T(0,t) - \theta(t))], \quad (35)$$

Here κ is the coefficient of thermal diffusivity, θ is the air temperature, λ is the coefficient of the surface-air heat transfer and c is specific heat. Although this equation has a formal closed form solution, for better physical interpretation we will start with the following simplification: since we are interested only in shallow waves, it is reasonable to ignore the energy dissipated in the depth of the soil/sand layer assuming that $Q_1 \ll Q_2$. Then the solution that satisfies Eq.(34) and the conditions (35) can be obtained as an instantaneous source

$$T(x,\eta,t-t_0) = \frac{E_s}{2c\rho_s\sqrt{\pi\kappa(t-t_0)}} \left\{ \left[e^{-\frac{(x-\eta)^2}{4\kappa(t-t_0)}} + e^{-\frac{(x+\eta)^2}{4\kappa(t-t_0)}} \right] - 2\lambda \int_0^{\infty} e^{-\frac{(x+\eta+\xi)^2}{4\kappa(t-t_0)}} e^{-\lambda\xi} d\xi \right\} + T_0, \quad (36)$$

representing the temperature at the point x at the time t if the heat $Q = c\rho$ is applied at initial time $t = t_0$. However, the problem with this solution is that the temperature at the point and time of the heat application is unbounded. In our case the heat is applied exactly to the surface, i.e. at $x = 0$, $t = t_0$ where t_0 is the time when the wave approaches the surface (see Eq.(22)). Therefore, according to our model, the surface temperature becomes unbounded at the time when the wave approaches it. Obviously, this formal mathematical result gives only qualitative description of the phenomenon. For quantitative physical interpretation of this result, one should depart from idealization of the soil/sand layer as a continuum by introducing a granular structure with the smallest length scale D equal to the diameter of a grain. Then instead of a single source (32) represented by a δ -function, one should apply a ‘‘thick’’ source uniformly distributed over the length D

$$Q_D = \frac{E_s}{D} \quad (37)$$

As a result, the temperature averaged over the thin layer of the thickness D is

$$T(0, t_0) = \frac{E_s}{c\rho D} + T_0, \quad (38)$$

After surpassing the singularity in the solution (36) by departing from the concept of the continuum, we can return to a slightly modified (homogeneous) version of Eq. (34) using the temperature (38) as the initial condition to the following problem

$$\frac{\partial T}{\partial t} = \kappa \frac{\partial^2 T}{\partial x^2}, \quad T(x, 0) = \frac{E_s}{c\rho D} + T_0, \quad 0 < x < D, \quad T(0, x) = T_0, D < x < \infty, \quad \frac{\partial T}{\partial x}(0, t) = 0 \quad (39)$$

For simplicity, the heat transfer from the surface to air has been ignored, i.e. $\lambda = 0$. The solution to Eq. (39) describing the evolution of the temperature profile over the soil/sand layer is

$$T(x, t) = \frac{E_s}{2c\rho D} \left[\operatorname{erf}\left(\frac{x+D}{2\sqrt{\kappa t}}\right) - \operatorname{erf}\left(\frac{x-D}{2\sqrt{\kappa t}}\right) \right] + T_0, \quad 0 \leq t < \infty \quad (40)$$

Hence, the evolution of the surface temperature is

$$T(0, t) = \frac{E_s}{c\rho D} \operatorname{erf}\left(\frac{D}{2\sqrt{\kappa t}}\right) + T_0, \quad 0 \leq t < \infty, \quad (41)$$

5. Energy balance.

As follows from Eq. (38), in order to find the surface temperature *prior* to a potential earthquake, one has to evaluate the energy E_s of the traveling shear waves. Occurrence of these waves depends upon several factors such as the stress build up (as a result of water transport, gas emissions, electric and magnetic fields, etc.), formation of material defects (dislocations, disclinations, vacancies), changes of local material properties under loading. Some of these factors are random; but even those of them that are deterministic, require precise knowledge of dynamical history of the specific area under consideration, and that history usually is not available. That is why we will turn to a global description of the dynamical evolution (based upon energy balance) with the purpose to evaluate the *order* of the surface temperature.

Prior to the earthquake, energy is accumulated in the form of the stress-based elastic potential. Due to different kind of perturbations, the potential energy is partly transferred into kinetic energy of elastic waves. These waves may include both compression and shear waves. After reflection from boundaries, compression waves can partly convert into shear waves, and vice versa. But the total mechanical energy is conserved unless there is dissipation “leak”. A soil/sand layer may represent such a leak: when shear wave approaches this layer, a small part of this wave (see Eq.(4)) penetrates it, and the energy transfers into heat. We will use the following typical value of potential energy per unit area (to be released during the earthquake)[8]:

$$E = \frac{4.13 \cdot 10^{14} J}{10^8 m^2} \quad (42)$$

Prior to the earthquake, a small portion of this energy dissipates into heat in the upper surface of the soil/sand layer. This portion has been evaluated in Eq. (4): for $H = 1\text{km}$,

$$E_s = 0.25 \cdot 10^{-3} E \quad (43)$$

Taking $D = 0.5\text{mm}$, and $c = 1000\text{ J/kgK}$, one obtains from (39) and (40) the increase of the surface temperature *prior* the earthquake:

$$\Delta T = \frac{4.13 \cdot 10^{14} \cdot 0.25 \cdot 10^{-3} J}{10^8 m^2 \cdot 0.5 \cdot 10^{-3} m \cdot 1.5 \cdot 10^3 kgm^{-3} \cdot 10^3 J/kgK} = 1.3^0 K \quad (44)$$

One should notice that this value is not to be taken in a precise way: there are several assumptions have been made that can change the result in both directions. For instance, firstly, it has been assumed that each shear wave approaches the soil/sand layer only once; actually after several reflections this wave can return and dissipate again, and that would double the dissipated energy in Eq. (43); obviously, it would double the increase of the temperature too. Secondly, the energy per unit area in Eq.(38) was averaged over the whole area subjected to the earthquake; however, at the epicenter of the expected earthquake, the values of this energy can be significantly higher, and that again would lead to higher surface temperature. At this stage we cannot offer more accurate evaluation, and therefore, it would be safe to interpret the result (44) as that the raise of the surface temperature is of *order of one degree K*.

6. Discussion.

There have been several attempts to explain the thermal anomaly on the free surface (such as fast appearance and disappearance of ground temperature increases) associated with pre-seismic activities [6]. In this study we concentrate on a special case when the area under consideration is covered by a layer of soil/sand of order of 1 km. The main specificity of this case is in the property of the free surface of such a layer: to absorb a traveling shear wave without reflection and with the energy dissipation at the very surface. In the following sub-sections we will discuss what kind of information about expected earthquake can be obtained from the observed thermal anomaly, and how this information can be extracted from the corresponding time series. We will also propose and discuss an experiment to verify the increase of surface temperature due to shear wave dissipation.

a) Inverse problem. In this sub-section we will discuss the following (inverse) problem: given the raise of the surface temperature (44), obtain maximum information about the expected earthquake. Assuming that all the physical and geometrical parameters in Eq.(44) are known, one can evaluate the energy per unit area E_s to be released during the expected earthquake. Obviously, the point on the surface where the raise of the temperature is the highest corresponds to the position of the epicenter, while the line on the surface along which the temperatures are observed approximates the position of the potential fault causing the expected earthquake. Further information is associated with the time-scales of the surface temperature evolution. The first time-scale follows directly from Eq.(41): in $\tau_1 = 16$ seconds the surface temperature $(T-T_0)$ drops at 90% of its initial value (given $\kappa = 4 \cdot 10^{-4} \text{ m}^2/\text{sec}$). Such a small time-scale (that is unusual for slow processes of thermal conductivity) is due to a small length scale $D=0.5 \text{ mm}$. The second time-scale is generated by elastic oscillations of shear waves reflecting from the potential fault and the border between the soil/sand layer. The period of these oscillations is of the order of $\tau_2 = 3 \text{ sec}$ (given the depth of the potential fault $b = 5 \text{ km}$, and the shear wave speed $v_r = 3400 \text{ m/sec}$). Since the thermal anomaly stays during hours, it is reasonable to

assume that the increase of the surface temperature is caused not by a single wave, but rather by a train of waves following each other with the time delays of order of τ_2 . For that case, the temperature evolution (41) should be modified as following

$$T(0,t) = \frac{E_s}{c\rho D} \sum_{j=1}^n \operatorname{erf}\left(\frac{D}{2\sqrt{\kappa(t-\tau_j)}}\right) + T_0, \quad 0 \leq t < \infty, \quad (45)$$

By fitting Eq. (45) into the observed time series, one can find E_s and τ_j . It should be noticed that the time delay τ defines the order of the depth b of the fault (namely, $b=0.5\tau v_r$). However, actually the problem is complicated by the fact that there are other sources of the surface temperature increase that are not associated with the earthquake (such as seasonal changes, as well as changes caused by man-made features). Therefore, the earthquake-related component of the surface temperature increase should be filter out of the mixture of other component. Let us assume that we know the Fourier transforms for each of these q components.

$$F_k = F_k(i\omega), \quad k = 1, 2, \dots, q, \quad (46)$$

Then the temperature evolution (45) can be sought in the form of its Fourier transform

$$F_0 = \frac{E_s}{c\rho Ds} \sum_{j=0}^n \exp(-\tau_j s) \left[1 - \exp\left(-\frac{2D\sqrt{s}}{\sqrt{\kappa}}\right)\right] + \frac{T_0}{s}, \quad s = i\omega \quad (47)$$

Introducing the weight coefficients a_k representing the portions of the partial Fourier power spectra of k -th components, one can write the following system of linear algebraic equations with respect to a_k

$$\sum_{k=0}^q a_k P_{ks} = P_s, \quad s = 1, 2, \dots, m, \quad P_{ks} = |F_{ks}(i\omega)|^2, \quad (48)$$

Here P_{ks} is the power of the spectrum of the k -th temperature component at the s -th frequency, P_s is the power of the spectrum of the observed temperature, and m is the number of frequencies at which the powers are assigned, Fig.4.

Thus we arrived at a system of q equations with respect to m unknowns. Usually q i.e. the number of different sources of the surface temperature increase, is of order of 10, while m , i.e. the number of frequencies at which the powers of the spectra are available, is of order of 100. Therefore, the system (48) is highly overdetermined, and its exact solution does not exist. However, one can find an approximate solution that is the "best fit" in a sense that the square root of the sum of squares of errors, i.e. the norm of the residual column-matrix, is minimal. This solution can be found, for instance, by applying a pseudoinverse $A^{(-1)}$ to the rectangular matrix $A = \|P_{ks}\|$ of the system (48)

$$|a_k| = A^{(-1)} |P_s|, \quad (49)$$

It should be noticed that unlike the power spectra P_{ks} ($s=1, 2, \dots, m$), that were assumed to be known, the sought power spectrum P_{0s} corresponding to the contribution of the shear-wave-generated temperature, is known only to accuracy of the knowledge of the temperature (44), and time delays τ_j . Hence, for the first approximation one has to assume that in Eq.(45)

$$\frac{E_s}{c\rho D} = T(0,0) = 1.3^0 K, \quad \tau_j = 3 \text{ sec} \quad (50)$$

that follows from the theoretical prediction of the order of these values. Then one has to turn to the residual column- matrix

$$|R_k| = AA^{(-1)} |P_s| - |P_k| \quad (51)$$

Its norm R that represents the error of the first approximation depends upon $T(0,0)=T^*$ and τ_j

$$R = R(T^*, \tau_j) \quad (52)$$

Obviously, the true values of T^* and τ_j , or to be more precise, their best-fit values, are supposed to minimize the norm (52). The minimization can be carried out by the gradient-decent algorithm coupled with the pseudoinverse solution (49).

Let us assume that the component a_0 representing the contribution of the shear-wave-generated temperature is small, i.e. $a_0 \ll 1$. That means that there is no indication of a pre-earthquake activity. On the contrary, if a_0 is of the same order as other components, the pre-earthquake activity as well as the configuration of the potential fault are detected. But in addition to that, based upon the optimal values of T^* and τ_j in Eq.(52), one can predict the order of the released power as well as the order of the depth of the fault of the expected earthquake. It should be emphasized that all the information extracted from the observed time series by solving the inverse problem is based upon the analytical model of the snap-of-a-whip phenomenon introduced in the previous sections

b) Proposed experiment. Experimental evidences of the snap-of-a-whip effect (spanned from a destructive power of a cable with a free end to a break-up of the sonic barrier at the end of a whip) have been known for centuries. The same effect has been recently observed during underground explosions when soil particles suffer a sudden jump over the free surface. However, an increase of the temperature associated with this effect has never been directly targeted. The objective of the proposed experiment is to verify and evaluate a significance of the temperature increase as a result of the shear wave dissipation at the free surface of sand rather than closely simulation of a specific natural condition .

The proposed experiment can be conducted using a tube (say, of height 2m, and radius 0.1m) made of a transparent non-magnetizable material. The tube is filled up by dry sand forming the upper free surface. A thin metallic disc with rough upper surface is submerged into sand (close to the bottom of the tube and concentric to its axis, but without any attachment to the tube). An electro-magnetic field applied to the submerged plate creates a variable axis-symmetrical torque that, in turn, generates rotational oscillations of the plate. Due to friction between sand and the plate, the oscillations lead to formation of the train of shallow shear waves that dissipate at the free surface. The temperature distribution over sand can be measured using infrared imaging camera providing accurate non-contact temperature measurements, Fig.5. It should be emphasized that the conditions of this experiment are different from the corresponding natural conditions. The difference is caused by unavoidable lateral boundaries (represented by the tube walls) that allow one to carry out the experiment within a reasonably limited space. However, in order to eliminate reflections from these

boundaries, one has to replace shear waves that, in natural conditions, are uniform in the lateral direction by the torsional shear waves similar to those in shafts. Nevertheless undesirable effects of walls are not totally eliminated: there are two types of additional

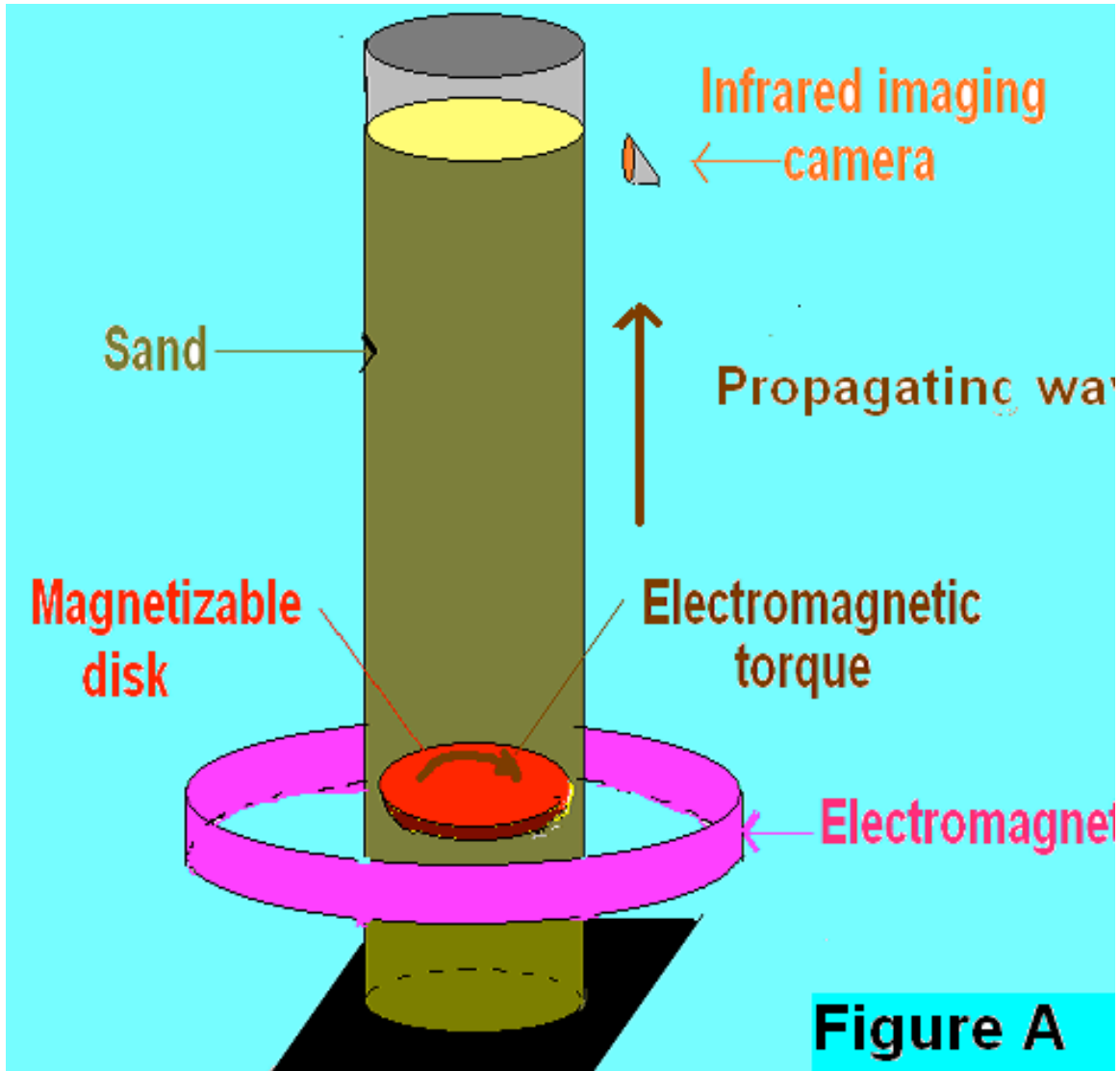


Figure A. Proposed experiment.

constraints imposed by these walls at the boundaries; no-slip condition and slip condition. The no-slip condition is similar to those at rigid boundary in viscous fluid

$$\frac{\partial u}{\partial t}(x, r = R, t) = 0 \quad \text{if} \quad \tau(x, r = R, t) < f_w g \rho x \quad (53)$$

Here r is current radial coordinate, R is radius of the tube, and f_w is the coefficient of friction between sand and the walls. This condition takes place when the sand pressure is sufficiently high, and therefore, the generated friction prevents sand from sliding with respect to the walls. Clearly it happens at the lower part of the tube. The slip condition takes place closer to the free surface when the pressure is small, and therefore the friction

cannot prevent sliding of sand with respect to the wall. This condition is formulated in term of shear stress

$$\tau(x, r = R, t) = f_w g \rho x \quad (54)$$

Thus, this model is slightly different from those described above: it is two-dimensional, and it includes additional energy dissipation via friction between sand and walls. Nevertheless, the qualitative effect of increase of the temperature at the free surface is supposed to be the same.

7. Conclusion.

A theory explaining thermal anomaly associated with pre-seismic activities for the areas where the ground is covered by a layer of soil or sand is proposed. It also explains why the temperature increase is observed only before and after, but not during the earthquake. The theory is based upon the snap-of-a-whip effect when a shear wave penetrates the upper soil/sand layer and releases its potential energy into heat at the very surface. A mathematical model that not only describes the phenomenon but also allows one to predict its parameters and dynamical characteristics has been derived. An experiment that would allow one to verify the effect of temperature increase due to the snap-of-a-whip effect has been proposed.

References.

1. Zak, M. Uniqueness and stability of the solution of the small perturbation problem of a flexible filament with a free end. PMM 39, 1048-1052, 1970, Moscow.
2. Zak, M. Cumulative effect at the soil surface due to shear wave propagation, Journal of Applied Mechanics 50, 227-228., 1983.
3. Zak, M. From Instability to Intelligence, pp 111-120, Springer, 1997.
4. Bryant, N., Zobrist, A., Logan, T., Precision automatic Co-Registration Procedure for NASA Sensors, (manuscript in preparation)
5. Bryant, N., Zobrist, A., Logan, T., Observed weather Satellite Thermal Responses Prior and After Earthquakes (manuscript in preparation).
6. Freund, F., Charge generation and Propagation in Igneous Rocks. Journal of Geodynamics, 33, 543-570, (2002).
7. Weigel, R., Earthquake Engineering, Prentice-Hall, Englewood Cliffs, N.J., 1970.
8. Turcotte, D., Geodynamics, Cambridge University Press. 2002 p 355.

